

Hyperbolic formulations and numerical relativity: II. asymptotically constrained systems of Einstein equations

Gen Yoneda¹ and Hisa-aki Shinkai²

¹ Department of Mathematical Sciences, Waseda University, Shinjuku, Tokyo, 169-8555, Japan

² Centre for Gravitational Physics and Geometry, 104 Davey Lab., Department of Physics, The Pennsylvania State University, University Park, PA 16802-6300, USA

E-mail: yoneda@mn.waseda.ac.jp and shinkai@gravity.phys.psu.edu

Received 27 July 2000, in final form 13 December 2000

Abstract

We study asymptotically constrained systems for numerical integration of the Einstein equations, which are intended to be robust against perturbative errors for the free evolution of the initial data. First, we examine the previously proposed ‘ λ system’, which introduces artificial flows to constraint surfaces based on the symmetric hyperbolic formulation. We show that this system works as expected for the wave propagation problem in the Maxwell system and in general relativity using Ashtekar’s connection formulation. Second, we propose a new mechanism to control the stability, which we call the ‘adjusted system’. This is simply obtained by adding constraint terms in the dynamical equations and adjusting their multipliers. We explain why a particular choice of multiplier reduces the numerical errors from non-positive or pure-imaginary eigenvalues of the adjusted constraint propagation equations. This ‘adjusted system’ is also tested in the Maxwell system and in the Ashtekar system. This mechanism affects more than the system’s symmetric hyperbolicity.

PACS numbers: 0420C, 0425, 0425D

(Some figures in this article are in colour only in the electronic version; see www.iop.org)

1. Introduction

Numerical relativity, an approach to solving the Einstein equations numerically, is supposed to be the only way to study highly nonlinear gravitational phenomena. Although the attempt already has decades of history, we still do not have a definite recipe for integrating the Einstein equations that will give us accurate and long-term stable time evolutions. Here and hereafter, we mean by ‘stable evolution’ that the system keeps the violation of the constraints within a suitable small value in its free numerical evolution.

As the authors discussed in our preceding paper (paper I) [1], one direction for obtaining a more stable system is to apply a set of dynamical equations which have a manifestly hyperbolic form (or first-order form). The standard Arnowitt–Deser–Misner (ADM) formulation does not have this feature, but there are many alternative proposals for constructing a hyperbolic set of equations [2–6], see also references in [1]. However, in paper I we showed that a symmetric hyperbolic form (mathematically, the ‘ultimate’ level of hyperbolicity) does not necessarily give the best performance for stable numerical evolution compared with weakly and strongly hyperbolic systems. This experiment was performed using Ashtekar’s connection variables [7], since this formulation enables us to compare three levels of hyperbolic formulations while keeping the same fundamental dynamical variables.

In this paper, we discuss different (but somewhat related) approaches to obtaining a stable evolution of the Einstein equations. The idea is to construct a system which is robust against the perturbative error produced during numerical time integration. We discuss the following two systems.

The first one is the so-called ‘ λ system’, which was proposed originally by Brodbeck, Frittelli, Hübner and Reula (BFHR) [8]. The idea of this approach is to introduce additional variables, λ , which indicates the violation of the constraints, and to construct a symmetric hyperbolic system for both the original variables and λ together with imposing dissipative dynamical equations for the λ s. BFHR constructed their λ system based on the Frittelli–Reula symmetric hyperbolic formulation of the Einstein equations [5], and we [9] have also presented a similar system for Ashtekar’s connection formulation [7] based on its symmetric hyperbolic expression [10, 11]. In section 2, we review this system and present numerical examples which show that this system behaves as expected.

The second one has the same motivation but turns out to be more practical, which we call an ‘adjusted system’. The essential procedure is to add constraint terms to the right-hand side of the dynamical equations with multipliers, and to choose the multipliers so as to decrease the violation of the constraint equations. This second step will be explained by obtaining non-positive or pure-imaginary eigenvalues of the adjusted constraint propagation equations. We note that adjusting the dynamical equation using the constraints is not a new idea. This can be seen, for example, in a remedial ADM system by Detweiler [12], in a conformally decoupled trace-free reformulation of ADM by Nakamura *et al* [13], and also in constructing hyperbolic formulations [2–5]. We also note that this eigenvalue criterion is also the core part of the theoretical support of the above λ system. In section 3, we describe this approach and present numerical examples, again in the Maxwell system and in the Ashtekar system.

This ‘adjusted system’ does not change the number of dynamical variables, and does not require hyperbolicity in the original set of equations. Therefore, we think that our results promote further applications in numerical relativity.

We will not repeat our explanation of Ashtekar’s connection formulation in our notation, nor of our detailed numerical procedures, since they are described in our paper I [1].

2. Asymptotically constrained system 1: λ system

We begin by reviewing the fundamental procedures of the ‘ λ system’ as proposed by Brodbeck *et al* [8]. We then demonstrate how this system works in Maxwell’s equations, and Ashtekar’s connection formulation of the Einstein equations in the following subsections.

2.1. The ‘ λ system’

The actual procedures for constructing a λ system are the following.

- (a) Prepare a symmetric hyperbolic evolution system which describes the problem; say

$$\partial_t u^\gamma = A^{i\gamma}_\delta \partial_i u^\delta + B^\gamma, \quad (2.1)$$

where u^γ ($\gamma = 1, \dots, N$) is a set of dynamical variables, $A(u(x^i))$ forms a symmetric matrix (Hermitian matrix when u is a complex variable) and $B(u(x^i))$ is a vector, where A and B do not include any further spatial derivatives in these components. The system may have constraint equations, which should be of first class. Ideally, we expect that the evolution equation of the set of constraints C^ρ ($\rho = 1, \dots, M$), which hereafter we denote by the constraint propagation equation, forms a first-order hyperbolic system (cf [14]), say

$$\partial_t C^\rho = D^{i\rho}_\sigma \partial_i C^\sigma + E^\rho_\sigma C^\sigma, \quad (2.2)$$

(where D, E are the same as A, B above) but this hyperbolicity may not be necessary.

- (b) Introduce λ^ρ as a measure of violation of the constraint equation, $C^\rho \approx 0$. (\approx denotes ‘weakly equal’). Here C^ρ is a given function of u and is assumed to be linear in its first-order space derivatives. We impose that λ obeys a dissipative equation of motion,

$$\partial_t \lambda^\rho = \alpha_{(\rho)} C^\rho - \beta_{(\rho)} \lambda^\rho \quad (\text{we do not sum over } \rho \text{ and } (\rho) \text{ on the right-hand side}) \quad (2.3)$$

with the initial data $\lambda^\rho = 0$, and by setting $\alpha \neq 0, \beta > 0$. We note that λ^ρ remains zero during the time evolution if there are no violations of the constraints.

- (c) Take a set (u, λ) of dynamical variables, and modify the evolution equations so as to form a symmetric hyperbolic system. That is, the set of equations

$$\partial_t \begin{pmatrix} u^\gamma \\ \lambda^\rho \end{pmatrix} \cong \begin{pmatrix} A^{i\gamma}_\delta & 0 \\ F^{i\rho}_\delta & 0 \end{pmatrix} \partial_i \begin{pmatrix} u^\delta \\ \lambda^\sigma \end{pmatrix}, \quad (2.4)$$

(\cong means that we have extracted only the term which appears in the principal part of the system) can be modified as

$$\partial_t \begin{pmatrix} u^\gamma \\ \lambda^\rho \end{pmatrix} \cong \begin{pmatrix} A^{i\gamma}_\delta & \bar{F}^i_{\sigma\gamma} \\ F^{i\rho}_\delta & 0 \end{pmatrix} \partial_i \begin{pmatrix} u^\delta \\ \lambda^\sigma \end{pmatrix}, \quad (2.5)$$

where the additional terms will not disturb the hyperbolicity of equations of u^γ , rather they make the whole system symmetric hyperbolic, which guarantees the well posedness of the system.

Therefore, the derived system, equation (2.5), should have a unique solution. If a perturbative violation of constraints, $\lambda^\rho \neq 0$, occurs during the evolution, by choosing appropriate α s and β s in (2.3), λ s can be made to decay to zero, which means that the total system evolves into the constraint surface asymptotically. We note that this procedure requires that the original system u forms a symmetric hyperbolic system, so that applications to the Einstein equations are somewhat restricted. BFHR [8] constructed this λ system using a Frittelli–Reula formulation [5]. We [9] also applied this system to the symmetric hyperbolic version of Ashtekar’s formulation [10].

We next review a brief proof of why the system (2.5) ensures that the evolution is constrained asymptotically. We first remark again that we only consider perturbative violations of constraints in our evolving system. The steps are the following.

- (a) Since we modify the equations for u^ν , the propagation equation of the constraints are also modified; write them schematically as

$$\partial_t C^\rho = D^{i\rho}{}_\sigma \partial_i C^\sigma + E^\rho{}_\sigma C^\sigma + G^{ij\rho}{}_\sigma \partial_i \partial_j \lambda^\sigma + H^{i\rho}{}_\sigma \partial_i \lambda^\sigma + I^\rho{}_\sigma \lambda^\sigma. \quad (2.6)$$

- (b) In order to see that the asymptotic behaviour of (λ^ρ, C^ρ) , we write them using their Fourier components so that their evolution equations take a homogenous form. That is, we transform (λ^ρ, C^ρ) to $(\hat{\lambda}^\rho, \hat{C}^\rho)$ as

$$\begin{aligned} \lambda(x, t)^\rho &= \int \hat{\lambda}(k, t)^\rho \exp(ik \cdot x) d^3k, \\ C(x, t)^\rho &= \int \hat{C}(k, t)^\rho \exp(ik \cdot x) d^3k. \end{aligned} \quad (2.7)$$

Then we see the evolution equations (2.3) and (2.6) become

$$\partial_t \begin{pmatrix} \hat{\lambda}^\rho \\ \hat{C}^\rho \end{pmatrix} = \begin{pmatrix} -\beta_{(\rho)} \delta_\sigma^\rho & \alpha_{(\rho)} \delta_\sigma^\rho \\ -G^{ij\rho}{}_\sigma k_i k_j + iH^{i\rho}{}_\sigma k_i + I^\rho{}_\sigma & iD^{i\rho}{}_\sigma k_i + E^\rho{}_\sigma \end{pmatrix} \begin{pmatrix} \hat{\lambda}^\sigma \\ \hat{C}^\sigma \end{pmatrix} =: P \begin{pmatrix} \hat{\lambda}^\sigma \\ \hat{C}^\sigma \end{pmatrix}. \quad (2.8)$$

- (c) If all eigenvalues of this coefficient matrix P have a negative real part, a pair $(\hat{\lambda}, \hat{C})$ evolves as $\exp(-\Lambda t)$ asymptotically where $-\Lambda$ is the diagonalized matrix of P , which indicates that the original variables (λ, C) evolves similarly. It would be best if we could determine the α and β in such a way in general, but it is not possible. Therefore, we extract the principal order of P and examine the condition for α and β so that P only has negative (real) eigenvalues. We remark again that this procedure is justified when we only consider a perturbative error from the constraint surface.

2.2. Example 1: Maxwell equations

As a first example, we present the Maxwell equations in a form of λ system. The Maxwell equations form linear and symmetric hyperbolic dynamical equations, together with two constraint equations, which might be the best system to start with.

2.2.1. λ system. The Maxwell equations for an electric field E^i and a magnetic field B^i in the vacuum consist of two constraint equations,

$$C_E := \partial_i E^i \approx 0, \quad (2.9)$$

$$C_B := \partial_i B^i \approx 0, \quad (2.10)$$

and a set of dynamical equations,

$$\partial_t \begin{pmatrix} E^i \\ B^i \end{pmatrix} = \begin{pmatrix} 0 & -c\epsilon^i{}_{j^l} \\ c\epsilon^i{}_{j^l} & 0 \end{pmatrix} \partial_l \begin{pmatrix} E^j \\ B^j \end{pmatrix}, \quad (2.11)$$

which satisfies symmetric hyperbolicity. The constraint evolutions become $\partial_t C_E = 0$ and $\partial_t C_B = 0$, which indicate (trivial) symmetric hyperbolicity. According to the above procedure, we introduce λ s which obey

$$\partial_t \lambda_E = \alpha_1 C_E - \beta_1 \lambda_E, \quad (2.12)$$

$$\partial_t \lambda_B = \alpha_2 C_B - \beta_2 \lambda_B, \quad (2.13)$$

with the initial data $\lambda_E = \lambda_B = 0$ and take $(E, B, \lambda_E, \lambda_B)$ as a set of variables to evolve:

$$\partial_t \begin{pmatrix} E^i \\ B^i \\ \lambda_E \\ \lambda_B \end{pmatrix} = \begin{pmatrix} 0 & -c\epsilon^i{}_j{}^l & 0 & 0 \\ c\epsilon^i{}_j{}^l & 0 & 0 & 0 \\ \alpha_1\delta^l{}_j & 0 & 0 & 0 \\ 0 & \alpha_2\delta^l{}_j & 0 & 0 \end{pmatrix} \partial_t \begin{pmatrix} E^j \\ B^j \\ \lambda_E \\ \lambda_B \end{pmatrix} + \begin{pmatrix} 0 \\ 0 \\ -\beta_1\lambda_E \\ -\beta_2\lambda_B \end{pmatrix}. \quad (2.14)$$

We immediately obtain an expected symmetric form as

$$\partial_t \begin{pmatrix} E^i \\ B^i \\ \lambda_E \\ \lambda_B \end{pmatrix} = \begin{pmatrix} 0 & -c\epsilon^i{}_j{}^l & \alpha_1\delta^{li} & 0 \\ c\epsilon^i{}_j{}^l & 0 & 0 & \alpha_2\delta^{li} \\ \alpha_1\delta^l{}_j & 0 & 0 & 0 \\ 0 & \alpha_2\delta^l{}_j & 0 & 0 \end{pmatrix} \partial_t \begin{pmatrix} E^j \\ B^j \\ \lambda_E \\ \lambda_B \end{pmatrix} + \begin{pmatrix} 0 \\ 0 \\ -\beta_1\lambda_E \\ -\beta_2\lambda_B \end{pmatrix}. \quad (2.15)$$

2.2.2. Analysis of eigenvalues. Now the evolution equations for the constraints C_E and C_B become

$$\partial_t C_E = \alpha_1(\Delta\lambda_E), \quad \partial_t C_B = \alpha_2(\Delta\lambda_B) \quad (2.16)$$

where $\Delta = \partial_i\partial^i$. We take the Fourier integrals for constraints C s (2.16) and λ s, (2.12) and (2.13), in the form of (2.7), to obtain

$$\partial_t \begin{pmatrix} \hat{C}_E \\ \hat{C}_B \\ \hat{\lambda}_E \\ \hat{\lambda}_B \end{pmatrix} = \begin{pmatrix} 0 & 0 & -\alpha_1 k^2 & 0 \\ 0 & 0 & 0 & -\alpha_2 k^2 \\ \alpha_1 & 0 & -\beta_1 & 0 \\ 0 & \alpha_2 & 0 & -\beta_2 \end{pmatrix} \begin{pmatrix} \hat{C}_E \\ \hat{C}_B \\ \hat{\lambda}_E \\ \hat{\lambda}_B \end{pmatrix}, \quad (2.17)$$

where $k^2 = k_i k^i$. We find the matrix to be constant. Note that this is an exact expression. Since the eigenvalues are

$$\left(-\beta_1 \pm \sqrt{\beta_1^2 - 4\alpha_1^2 k^2}\right)/2$$

and

$$\left(-\beta_2 \pm \sqrt{\beta_2^2 - 4\alpha_2^2 k^2}\right)/2,$$

the negative eigenvalue requirement becomes $\alpha_1, \alpha_2 \neq 0$ and $\beta_1, \beta_2 > 0$.

2.2.3. Numerical demonstration. We present a numerical demonstration of the above Maxwell ‘ λ system’. We prepare a code which produces electromagnetic propagation in the x - y -plane, and monitor the violation of the constraint during time integration. Specifically, we prepare the initial data with a Gaussian packet at the origin,

$$E^i(x, y, z) = (-Ay e^{-B(x^2+y^2)}, Ax e^{-B(x^2+y^2)}, 0), \quad (2.18)$$

$$B^i(x, y, z) = (0, 0, 0), \quad (2.19)$$

where A and B are constants, and let it propagate freely, under the periodic boundary condition.

The code itself is quite stable for this problem. In figure 1, we plot the L2 norm of the error (C_E over the whole grid) as a function of time. The full curve (constant) in figure 1(a) is of the original Maxwell equation. If we introduce λ s, then we see that the error will be reduced by a particular choice of α and β . Figure 1(a) is for changing α with $\beta = 2.0$,

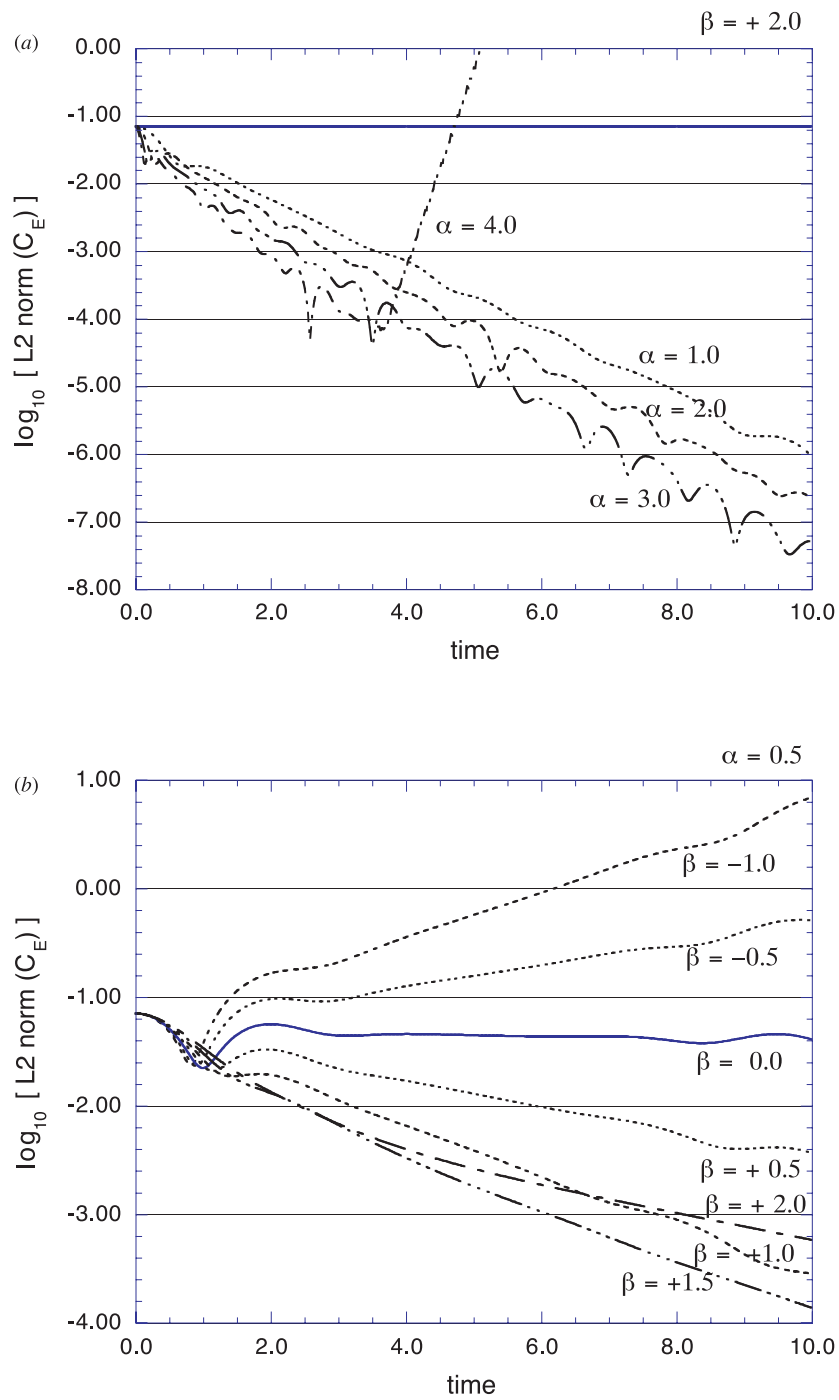


Figure 1. Demonstration of the λ system in the Maxwell equation. (a) Constraint violation (L2 norm of C_E) versus time with constant β ($= 2.0$) but changing α . Here $\alpha = 0$ means no λ system. (b) The same plot with constant α ($= 0.5$) but changing β . We see better performance for $\beta > 0$, which is the case of negative eigenvalues of the constraint propagation equation. The constants in (2.18) were chosen as $A = 200$ and $B = 1$.

while figure 1(b) is for changing β with $\alpha = 0.5$. Here, we simply use $\alpha := \alpha_1 = \alpha_2$ and $\beta := \beta_1 = \beta_2$. We see better performance for $\beta > 0$ (figure 1(b)), which is the case of negative eigenvalues of the constraint propagation equation. We also see that the system will diverge for large α (figure 1(b)). The upper bound of α can be explained by the violation of the Courant–Friedrich–Lewy (CFL) condition, where the characteristic speed comes from the flux term of the dynamical equations (2.15).

2.3. Example 2: Einstein equations (Ashtekar equations)

The second demonstration is of the vacuum Einstein equations in Ashtekar’s connection formalism [7].

Before going through the λ system, we will briefly outline the equations. The fundamental Ashtekar variables are the densitized inverse triad, \tilde{E}_a^i , and the $SO(3, C)$ self-dual connection, \mathcal{A}_i^a , where the indices i, j, \dots indicate the 3-spacetime, and a, b, \dots is for $SO(3)$ space. The total four-dimensional spacetime is described together with the gauge variables $\tilde{N}, N^i, \mathcal{A}_0^a$, which we call the densitized lapse function, shift vector and the triad lapse function. Since the Hilbert action takes the form

$$S = \int d^4x [(\partial_t \mathcal{A}_i^a) \tilde{E}_a^i + \tilde{N} \mathcal{C}_H + N^i \mathcal{C}_{Mi} + \mathcal{A}_0^a \mathcal{C}_{Ga}], \quad (2.20)$$

the system has three constraint equations, $\mathcal{C}_H \approx \mathcal{C}_{Mi} \approx \mathcal{C}_{Ga} \approx 0$, which are called the Hamiltonian, momentum and Gauss constraint equation, respectively. They are written as

$$\mathcal{C}_H := (i/2) \epsilon^{ab} \tilde{E}_a^i \tilde{E}_b^j F_{ij}^c, \quad (2.21)$$

$$\mathcal{C}_{Mi} := -F_{ij}^a \tilde{E}_a^j, \quad (2.22)$$

$$\mathcal{C}_{Ga} := \mathcal{D}_i \tilde{E}_a^i, \quad (2.23)$$

where $F_{\mu\nu}^a := 2\partial_{[\mu} \mathcal{A}_{\nu]}^a - i\epsilon^{abc} \mathcal{A}_\mu^b \mathcal{A}_\nu^c$ is the curvature 2-form and $\mathcal{D}_i \tilde{E}_a^j := \partial_i \tilde{E}_a^j - i\epsilon_{abc} \mathcal{A}_i^b \tilde{E}_c^j$. The original dynamical equation for $(\tilde{E}_a^i, \mathcal{A}_i^a)$ constitutes a weakly hyperbolic form,

$$\partial_t \tilde{E}_a^i = -i\mathcal{D}_j (\epsilon^{cb} \tilde{N} \tilde{E}_c^j \tilde{E}_b^i) + 2\mathcal{D}_j (N^{[j} \tilde{E}_a^{i]}) + i\mathcal{A}_0^b \epsilon_{ab}^c \tilde{E}_c^i, \quad (2.24)$$

$$\partial_t \mathcal{A}_i^a = -i\epsilon^{ab} \tilde{N} \tilde{E}_b^j F_{ij}^c + N^j F_{ji}^a + \mathcal{D}_i \mathcal{A}_0^a \quad (2.25)$$

where $\mathcal{D}_j X_a^{ji} := \partial_j X_a^{ji} - i\epsilon_{abc} \mathcal{A}_j^b X_c^{ji}$, for $X_a^{ij} + X_a^{ji} = 0$. It is also possible to express (2.24) and (2.25) to reveal symmetric hyperbolicity [10, 11]. For more detailed definitions and our notation, please see appendix A of our paper I [1].

2.3.1. λ system for controlling constraint violations. Here, we only consider the λ system which controls the violation of the constraint equations. In [9], we have also discussed an advanced version of the λ system which controls the violations of the reality condition.

We introduce new variables $(\lambda, \lambda_i, \lambda_a)$, obeying the dissipative evolution equations,

$$\partial_t \lambda = \alpha_1 C_H - \beta_1 \lambda, \quad (2.26)$$

$$\partial_t \lambda_i = \alpha_2 \tilde{C}_{Mi} - \beta_2 \lambda_i, \quad (2.27)$$

$$\partial_t \lambda_a = \alpha_3 C_{Ga} - \beta_3 \lambda_a, \quad (2.28)$$

where $\alpha_i \neq 0$ (possibly complex) and $\beta_i > 0$ (real) are constants.

If we take $y_\alpha := (\tilde{E}_a^i, \mathcal{A}_i^a, \lambda, \lambda_i, \lambda_a)$ as a set of dynamical variables, then the principal part of (2.26)–(2.28) can be written as

$$\partial_t \lambda \cong -i\alpha_1 \epsilon^{bcd} \tilde{E}_c^j \tilde{E}_d^l (\partial_l \mathcal{A}_j^b), \quad (2.29)$$

$$\partial_t \lambda_i \cong \alpha_2 [-e \delta_i^l \tilde{E}_b^j + e \delta_i^j \tilde{E}_b^l] (\partial_l \mathcal{A}_j^b), \quad (2.30)$$

$$\partial_t \lambda_a \cong \alpha_3 \partial_l \tilde{E}_a^l. \quad (2.31)$$

The characteristic matrix of the system u_α is not Hermitian. However, if we modify the right-hand side of the evolution equation of $(\tilde{E}_a^i, \mathcal{A}_i^a)$, then the set becomes a symmetric hyperbolic system. This is done by adding $\bar{\alpha}_3 \gamma^{il} (\partial_l \lambda_a)$ to the equation of $\partial_t \tilde{E}_a^i$, and by adding $i\bar{\alpha}_1 \epsilon^{abcd} \tilde{E}_i^c \tilde{E}_d^l (\partial_l \lambda) + \bar{\alpha}_2 (-e \gamma^{lm} \tilde{E}_i^a + e \delta_i^m \tilde{E}^{la}) (\partial_l \lambda_m)$ to the equation of $\partial_t \mathcal{A}_i^a$. The final principal part is then written as

$$\begin{aligned} & \partial_t \begin{pmatrix} \tilde{E}_a^i \\ \mathcal{A}_i^a \\ \lambda \\ \lambda_i \\ \lambda_a \end{pmatrix} \\ & \cong \begin{pmatrix} \mathcal{M}^l{}_a{}^{bi}{}_j & 0 & 0 & 0 & \bar{\alpha}_3 \gamma^{il} \delta_a^b \\ 0 & \mathcal{N}^l{}_i{}^a{}_b{}^j & i\bar{\alpha}_1 \epsilon^{abcd} \tilde{E}_i^c \tilde{E}_d^l & \bar{\alpha}_2 e (\delta_i^j \tilde{E}^{la} - \gamma^{lj} \tilde{E}_i^a) & 0 \\ 0 & -i\alpha_1 \epsilon_b{}^{cd} \tilde{E}_c^j \tilde{E}_d^l & 0 & 0 & 0 \\ 0 & \alpha_2 e (\delta_i^j \tilde{E}_b^l - \delta_i^l \tilde{E}_b^j) & 0 & 0 & 0 \\ \alpha_3 \delta_a^b \delta_j^l & 0 & 0 & 0 & 0 \end{pmatrix} \\ & \quad \times \partial_l \begin{pmatrix} \tilde{E}_b^j \\ \mathcal{A}_j^b \\ \lambda \\ \lambda_j \\ \lambda_b \end{pmatrix}, \end{aligned} \quad (2.32)$$

where

$$\mathcal{M}^{labij} = i\epsilon^{abc} \tilde{N} \tilde{E}_c^l \gamma^{ij} + N^l \gamma^{ij} \delta^{ab}, \quad (2.33)$$

$$\begin{aligned} \mathcal{N}^{labij} = & i\tilde{N} (\epsilon^{abc} \tilde{E}_c^j \gamma^{li} - \epsilon^{abc} \tilde{E}_c^l \gamma^{ji} - e^{-2} \tilde{E}^{ia} \epsilon^{bcd} \tilde{E}_c^j \tilde{E}_d^l - e^{-2} \epsilon^{acd} \tilde{E}_d^l \tilde{E}_c^l \tilde{E}^{jb} \\ & + e^{-2} \epsilon^{acd} \tilde{E}_d^i \tilde{E}_c^j \tilde{E}^{lb}) + N^l \delta^{ab} \gamma^{ij}. \end{aligned} \quad (2.34)$$

Clearly, the solution $(\tilde{E}_a^i, \mathcal{A}_i^a, \lambda, \lambda_i, \lambda_a) = (\tilde{E}_a^i, \mathcal{A}_i^a, 0, 0, 0)$ represents the original solution of the Ashtekar system.

2.3.2. *Analysis of eigenvalues.* After linearizing and taking the Fourier transformation (2.7), the propagation equation of the constraints ($\mathcal{C}_H, \tilde{\mathcal{C}}_{Mi}, \mathcal{C}_{Ga}$) and $(\lambda, \lambda_i, \lambda_a)$ is written as

$$\partial_t \begin{pmatrix} \hat{\mathcal{C}}_H \\ \tilde{\hat{\mathcal{C}}}_{Mi} \\ \hat{\mathcal{C}}_{Ga} \\ \hat{\lambda} \\ \hat{\lambda}_i \\ \hat{\lambda}_a \end{pmatrix} = \begin{pmatrix} 0 & -ik_j & 0 & -2\bar{\alpha}_1 k_m k^m & 0 & 0 \\ -ik_i & k_m \epsilon^m{}_i{}^j & 0 & 0 & -\bar{\alpha}_2 (k_i k^j + k_m k^m \delta_i^j) & 0 \\ 0 & -2\delta_a^b & \epsilon^{mb}{}_a k_m & 2i\bar{\alpha}_1 k_a & \bar{\alpha}_2 \epsilon^{amj} k_m & -\bar{\alpha}_3 k_m k^m \delta_a^b \\ \alpha_1 & 0 & 0 & -\beta_1 & 0 & 0 \\ 0 & \alpha_2 \delta_i^j & 0 & 0 & -\beta_2 \delta_i^j & 0 \\ 0 & 0 & \alpha_3 \delta_a^b & 0 & 0 & -\beta_3 \delta_a^b \end{pmatrix} \times \begin{pmatrix} \hat{\mathcal{C}}_H \\ \tilde{\hat{\mathcal{C}}}_{Mj} \\ \hat{\mathcal{C}}_{Gb} \\ \hat{\lambda} \\ \hat{\lambda}_j \\ \hat{\lambda}_b \end{pmatrix}. \quad (2.35)$$

In order to link the discussion with our later demonstration in the plane-symmetric spacetime, here we only consider the Fourier component of $k_i = (1, 0, 0)$ for simplicity. The eigenvalues, E_i ($i = 1, \dots, 14$), of the characteristic matrix of (2.35) can be written explicitly as

$$(E_1, \dots, E_{10}) = \begin{cases} -\frac{1}{2}\beta_3 \pm \frac{1}{2}\sqrt{\beta_3^2 - 4|\alpha_3|^2}, \\ -\frac{1}{2}(i + \beta_3) \pm \frac{1}{2}\sqrt{-1 - 4|\alpha_3|^2 - 2i\beta_3 + \beta_3^2}, \\ -\frac{1}{2}(-i + \beta_3) \pm \frac{1}{2}\sqrt{-1 - 4|\alpha_3|^2 - 2i\beta_3 + \beta_3^2}, \\ -\frac{1}{2}(i + \beta_2) \pm \frac{1}{2}\sqrt{-1 - 4|\alpha_2|^2 - 2i\beta_2 + \beta_2^2}, \\ -\frac{1}{2}(-i + \beta_2) \pm \frac{1}{2}\sqrt{-1 - 4|\alpha_2|^2 - 2i\beta_2 + \beta_2^2} \end{cases}$$

and as solutions (E_{11}, \dots, E_{14}) of the quartic equation

$$x^4 + (\beta_2 + \beta_1)x^3 + (2|\alpha_1|^2 + 2|\alpha_2|^2 + 1 + \beta_1\beta_2)x^2 + (2|\alpha_2|^2\beta_1 + \beta_2 + \beta_1 + 2|\alpha_1|^2\beta_2)x + (\beta_1\beta_2 + 4|\alpha_1|^2|\alpha_2|^2) = 0, \quad (2.36)$$

where $|\alpha_i|^2 = \alpha_i \bar{\alpha}_i$. We omit the explicit expressions of E_{11}, \dots, E_{14} in order to save space.

A possible set of conditions on α_ρ, β_ρ ($\rho = 1, 2, 3$) for $\text{Re } e(E_i) < 0$ are

$$\alpha_\rho \neq 0 \quad \text{and} \quad \beta_\rho > 0. \quad (2.37)$$

This is true (necessary and sufficient) for E_1, \dots, E_{10} , and also plausible for E_{11}, \dots, E_{14} as far as our numerical evaluation tells us (see figure 2).

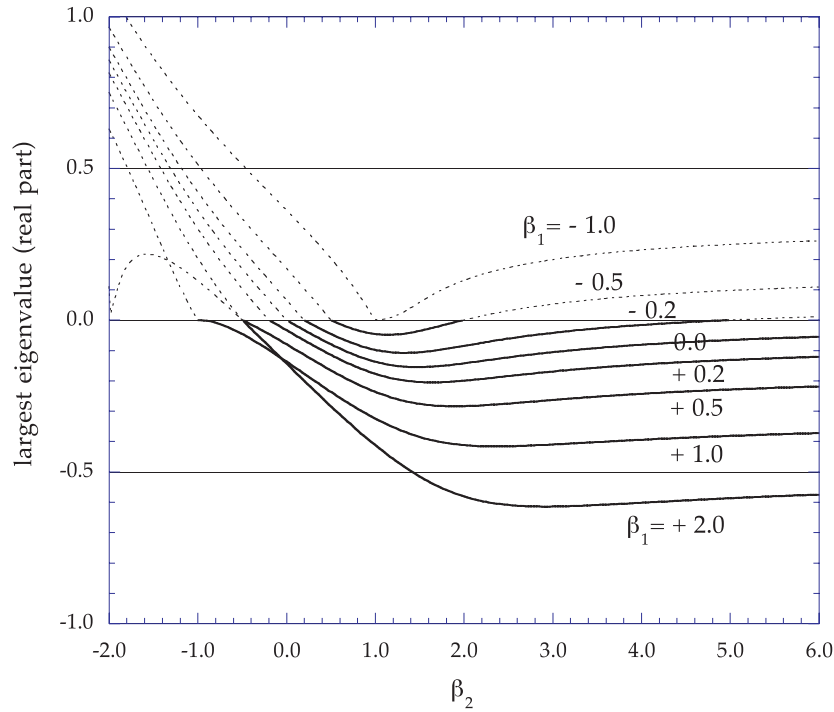


Figure 2. Example of eigenvalues of the system (2.35). We plot the eigenvalue which has the maximum real part between four of them, for the case of fixing $\alpha_1 = \alpha_2 = 1$ and changing β_1 and β_2 . We see that our desired condition, ‘all negative real eigenvalues’, is available when the combinations produce the full curves. That is, when both β take large positive values.

2.3.3. Numerical demonstration. In this subsection, we demonstrate that the λ system for the Ashtekar equation actually works as expected.

The model we present here is gravitational wave propagation in a planar spacetime under periodic boundary conditions. We perform a full numerical simulation using Ashtekar’s variables. We prepare two +-mode strong pulse waves initially by solving the ADM Hamiltonian constraint equation, using the York–O’Murchadha conformal approach. Then we transform the initial Cauchy data (3-metric and extrinsic curvature) into the connection variables, $(\tilde{E}_a^i, \mathcal{A}_i^a)$, and evolve them using the dynamical equations. For the presentation in this paper, we apply the geodesic slicing condition (ADM lapse $N = 1$, with zero shift and zero triad lapse). We have used both the Brailovskaya integration scheme, which is a second-order predictor–corrector method, and the so-called iterative Crank–Nicholson integration scheme for numerical time evolutions. The details of the numerical method are described in paper I [1], where we also described how our code shows second-order convergence behaviour.

In order to show the expected ‘stabilization behaviour’ clearly, we artificially add an error in the middle of the time evolution. More specifically, we set our initial guess 3-metric as

$$\hat{\gamma}_{ij} = \begin{pmatrix} 1 & 0 & 0 \\ \text{sym} & 1 + K(e^{-(x-L)^2} + e^{-(x+L)^2}) & 0 \\ \text{sym} & \text{sym} & 1 - K(e^{-(x-L)^2} + e^{-(x+L)^2}) \end{pmatrix}, \quad (2.38)$$

in the periodically bounded region $x = [-5, +5]$, and added an artificial inconsistent rescaling

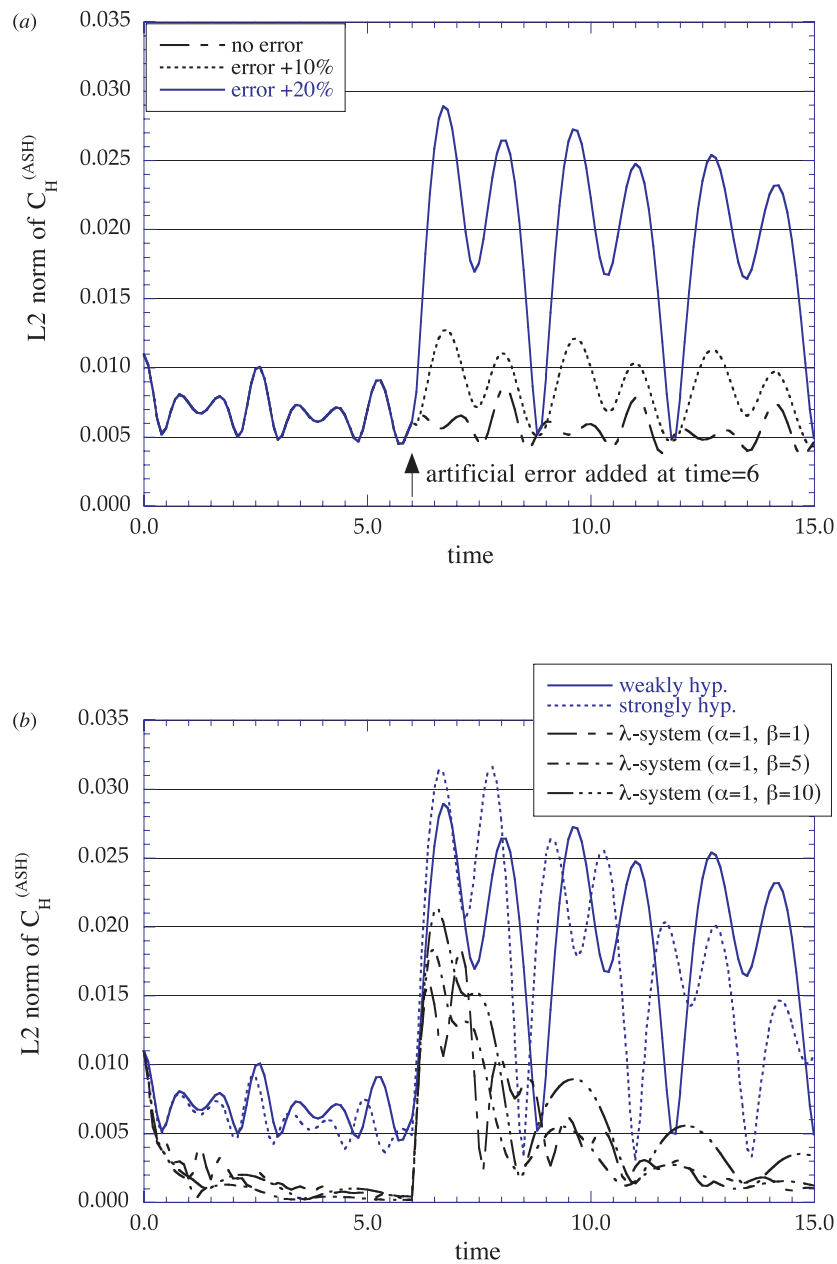


Figure 3. Demonstration of the λ system in the Ashtekar equation. We plot the violation of the constraint (the L2 norm of the Hamiltonian constraint equation, C_H) for the cases of plane-wave propagation under the periodic boundary. To see the effect more clearly, we added an artificial error at $t = 6$. Part (a) shows how the system goes bad depending on the amplitude of artificial error. The error was of the form $\mathcal{A}_y^2 \rightarrow \mathcal{A}_y^2(1 + \text{error})$. All the curves are of the evolution of Ashtekar's original equation (no λ system). Part (b) shows the effect of the λ system. All the curves have 20% error amplitude, but show the difference of the evolution equations. The full curve is for Ashtekar's original equation (the same as in (a)), the dotted curve is for the strongly hyperbolic Ashtekar equation. Other curves are of λ systems, which produce a better performance than that of the strongly hyperbolic system.

once at time $t = 6$ for the \mathcal{A}_y^2 component as $\mathcal{A}_y^2 \rightarrow \mathcal{A}_y^2(1 + \text{error})$. Here K and L are constants and we set $K = 0.3$ and $L = 2.5$ for the plots.

Figure 3(a) shows how the violation of the Hamiltonian constraint equation, \mathcal{C}_H , becomes worse depending on the error term. The oscillation of the L2 norm \mathcal{C}_H in the figure due to the pulse waves collide periodically in the numerical region. We, then, fix the error term as a 20% spike, and try to evolve the same data in different equations of motion, i.e. the original Ashtekar equation (full curve in figure 3(b)), the strongly hyperbolic version of Ashtekar's equation (dotted curve) and the above λ system equation (other curves) with different β s but the same α . As we expected, all the λ system cases result in reducing the Hamiltonian constraint errors.

2.4. Remarks for the λ system

In the previous subsections, we showed that the λ system works as we expected. The system evolves into a constraint surface asymptotically even if we added an error artificially. However, the λ system cannot be introduced generally, because (a) the construction of the λ system requires that the original dynamical equation be in symmetric hyperbolic form, which is quite restrictive for the Einstein equations, and (b) the system requires many additional variables and we also need to evaluate all the constraint equations at every time step, which is a hard computational task. Moreover, it is not clear that the λ system can control constraint equations which do not have any spatial differential terms (e.g. the primary metric reality condition in the Ashtekar formulation³).

Next, we propose an alternative system which also enables us to control the violation of the constraint equations, but is robust for the above points.

3. Asymptotically constrained system 2: adjusted system

Here we propose another approach to obtaining stable evolutions, which we call the 'adjusted system'. The essential procedure is to add constraint terms to the right-hand side of the dynamical equations with multipliers, and to choose the multipliers so that the adjusted equations decrease the violation of constraints during time evolution. This system has several advantages over the previous λ system.

3.1. 'Adjusted system'

The actual procedure for constructing an adjusted system is as follows.

- (1) Prepare a set of evolution equations for dynamical variables and the first-class constraints which describe the problem. It is not required that the system be in the first-order form or hyperbolic form. However, here we start from the same form with (2.1) and (2.2). We repeat them as

$$\partial_t u^\gamma = A^{i\gamma}{}_\delta \partial_i u^\delta + B^\gamma, \quad (3.1)$$

$$\partial_t C^\rho = D^{i\rho}{}_\sigma \partial_i C^\sigma + E^\rho{}_\sigma C^\sigma, \quad (3.2)$$

where $A(u(x^i))$ is not required to form a symmetric or Hermitian matrix.

³ This statement is not inconsistent with our previous work [9], in which we also proposed a λ system that can control the *secondary triad* reality condition.

- (2) Add the constraint terms, C^ρ (and/or their derivatives) to the dynamical equation (3.1) with multipliers κ ,

$$\partial_t u^\gamma = A^{i\gamma}{}_\delta \partial_i u^\delta + B^\gamma + \kappa_\rho^\gamma C^\rho + \kappa_\rho^{\gamma i} \partial_i C^\rho. \quad (3.3)$$

We call the added terms, $\kappa_\rho^\gamma C^\rho$ and/or $\kappa_\rho^{\gamma i} \partial_i C^\rho$, ‘adjusted terms’, and leave κ_ρ^γ and $\kappa_\rho^{\gamma i}$ unspecified for the moment. Because of these adjusted terms, the original constraint propagation equations, (3.2), must also be adjusted:

$$\partial_t C^\rho = D^{i\rho}{}_\sigma \partial_i C^\sigma + E^\rho{}_\sigma C^\sigma + F^{ij\rho}{}_\sigma \partial_i \partial_j C^\sigma + G^{i\rho}{}_\sigma \partial_i C^\sigma + H^\rho{}_\sigma C^\sigma. \quad (3.4)$$

The last three terms are due to the adjusted terms.

- (3) Specify the multipliers κ , by evaluating the eigenvalues that appear on the right-hand side of (3.4). Practically, by taking the Fourier transformation (2.7), we can reduce (3.4) to a homogeneous form,

$$\partial_t \hat{C}^\rho = (ik_i D^{i\rho}{}_\sigma + E^\rho{}_\sigma - k_i k_j F^{ij\rho}{}_\sigma + ik_i G^{i\rho}{}_\sigma + H^\rho{}_\sigma) \hat{C}^\sigma. \quad (3.5)$$

We then take a linearization against a certain background spacetime,

$$\partial_t {}^{(1)}\hat{C}^\rho = (ik_i {}^{(0)}D^{i\rho}{}_\sigma + {}^{(0)}E^\rho{}_\sigma - k_i k_j {}^{(0)}F^{ij\rho}{}_\sigma + ik_i {}^{(0)}G^{i\rho}{}_\sigma + {}^{(0)}H^\rho{}_\sigma) {}^{(1)}\hat{C}^\sigma, \quad (3.6)$$

(here (n) indicates the order in linearization) and evaluate the eigenvalues of the coefficient matrix in (3.6).

For this process, we propose two guidelines.

- (a) The first one is to obtain the *negative* real part of the eigenvalues. This is from the same principle in the λ system when we specified α and β , in order to force the system to approach the constraint surface asymptotically. Provided that we obtain κ which produces all the negative real part eigenvalues, the Fourier component \hat{C} decays to zero in time evolution, and so does the original constraint term C .
- (b) An alternative guideline is to obtain as many *non-zero* eigenvalues as one can. More precisely, this case is supposed to have *pure imaginary* eigenvalues. In such a case, the constraint propagation equations (e.g. $\partial_t \hat{C} = \pm ik \hat{C}$) behave like the normal wave equations in its original component (e.g. $\partial_t C = \pm \partial_x C$), and its stability can be discussed using von Neumann stability analysis. As is well known, stability depends on the choice of numerical integration scheme, but it is also certain that we can control (or decrease) the amplitude of the constraint terms.

The advantage of this adjusted system is that we do not need to add variables to the fundamental set, while the above first guideline (3a) is the same mechanism as applied for the λ system. We note that the *non-zero* eigenvalue feature was conjectured in Alcubierre *et al* [15] in order to show the advantage of the conformally scaled ADM system, but the discussion there is of dynamical equations and not of constraint propagation equations.

Guideline (3b) is obtained heuristically as we will show in figure 5 that a system with three zero eigenvalues is more stable than one with five. However, we conjecture that systems with non-zero (or pure-imaginary) eigenvalues in their constraint propagation equations have more dissipative features than that of the zero-eigenvalue system. This is from the von Neumann stability analysis, evaluating dynamical variables with the finite-differenced quantities (see appendix B for more details).

We note that adding constraint terms to the dynamical equations is not a new idea. For example, Detweiler [12] applied this procedure to the ADM equations and used the finiteness of the norm to obtain a new system. This is also one of the standard procedures for constructing

a symmetric hyperbolic system (e.g. [2–5, 10]). We believe, however, that the above guidelines yield the essential mechanism for our purpose of constructing a stable dynamical system.

In the following subsections and appendix A, we demonstrate that this adjusted system actually works as desired in the Maxwell system and in the Ashtekar system of the Einstein equations, in which the above two guidelines are applied, respectively.

3.2. Example 1: Maxwell equations

3.2.1. Adjusted system. Here we again consider the Maxwell equations (2.9)–(2.11). We start from the adjusted dynamical equations

$$\partial_t E_i = c\epsilon_i^{jk}\partial_j B_k + P_i C_E + p^j{}_i(\partial_j C_E) + Q_i C_B + q^j{}_i(\partial_j C_B), \quad (3.7)$$

$$\partial_t B_i = -c\epsilon_i^{jk}\partial_j E_k + R_i C_E + r^j{}_i(\partial_j C_E) + S_i C_B + s^j{}_i(\partial_j C_B), \quad (3.8)$$

where P, Q, R, S, p, q, r and s are multipliers. These dynamical equations adjust the constraint propagation equations as

$$\begin{aligned} \partial_t C_E &= (\partial_i P^i)C_E + P^i(\partial_i C_E) + (\partial_i Q^i)C_B + Q^i(\partial_i C_B) \\ &\quad + (\partial_i p^{ji})(\partial_j C_E) + p^{ji}(\partial_i \partial_j C_E) + (\partial_i q^{ji})(\partial_j C_B) + q^{ji}(\partial_i \partial_j C_B), \end{aligned} \quad (3.9)$$

$$\begin{aligned} \partial_t C_B &= (\partial_i R^i)C_E + R^i(\partial_i C_E) + (\partial_i S^i)C_B + S^i(\partial_i C_B) \\ &\quad + (\partial_i r^{ji})(\partial_j C_E) + r^{ji}(\partial_i \partial_j C_E) + (\partial_i s^{ji})(\partial_j C_B) + s^{ji}(\partial_i \partial_j C_B). \end{aligned} \quad (3.10)$$

This will be expressed using Fourier components by

$$\begin{aligned} \partial_t \begin{pmatrix} \hat{C}_E \\ \hat{C}_B \end{pmatrix} &= \begin{pmatrix} \partial_i P^i + iP^i k_i + ik_j(\partial_i p^{ji}) - k_i k_j p^{ji} & \partial_i Q^i + iQ^i k_i + ik_j(\partial_i q^{ji}) - k_i k_j q^{ji} \\ \partial_i R^i + iR^i k_i + ik_j(\partial_i r^{ji}) - k_i k_j r^{ji} & \partial_i S^i + iS^i k_i + ik_j(\partial_i s^{ji}) - k_i k_j s^{ji} \end{pmatrix} \\ &\quad \times \begin{pmatrix} \hat{C}_E \\ \hat{C}_B \end{pmatrix} =: T \begin{pmatrix} \hat{C}_E \\ \hat{C}_B \end{pmatrix}. \end{aligned} \quad (3.11)$$

Assuming the multipliers are constants or functions of E and B , we can truncate the principal matrix as

$${}^{(0)}T = \begin{pmatrix} iP^i k_i - k_i k_j p^{ji} & iQ^i k_i - k_i k_j q^{ji} \\ iR^i k_i - k_i k_j r^{ji} & iS^i k_i - k_i k_j s^{ji} \end{pmatrix}, \quad (3.12)$$

with eigenvalues

$$\Lambda^\pm = \frac{p + s \pm \sqrt{p^2 + 4qr - 2ps + s^2}}{2}, \quad (3.13)$$

where $p := iP^i k_i - k_i k_j p^{ji}$, $q := iQ^i k_i - k_i k_j q^{ji}$, $r := iR^i k_i - k_i k_j r^{ji}$, $s := iS^i k_i - k_i k_j s^{ji}$.

If we fix $q = r = 0$, then $\Lambda^\pm = p, s$. Furthermore, if we assume $p^{ji}, s^{ji} > 0$, and set everything else to zero, then $\Lambda^\pm < 0$, that is we can get all the eigenvalues which have a negative real part. That is, our guideline (a) is satisfied. (Conversely, if we choose $q = r = 0$ and $p^{ji}, s^{ji} < 0$, then $\Lambda^\pm > 0$.)

3.2.2. Numerical demonstration. We applied the above adjusted system to the same wave propagation problem as in section 2.2.3. For simplicity, we fix $\kappa = p^{ij} = s^{ij}$ and set other multipliers equal to zero. In figure 4, we show the L2 norm of the constraint violation as a function of time, with various κ . As was expected, we see better performance for $\kappa > 0$ (of the system with a negative real part of the constraint propagation equation), while diverging behaviour for $\kappa < 0$ (of the system with a positive real part of the constraint propagation equation).

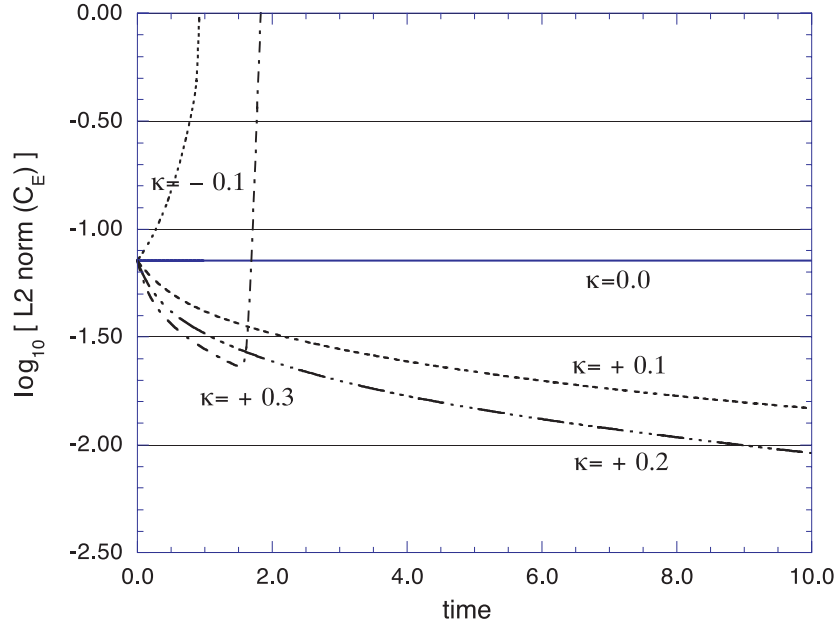


Figure 4. Demonstrations of the adjusted system in the Maxwell equation. We perform the same experiments with section 2.2.3 (figure 1). Constraint violation (L2 norm of C_E) versus time are plotted for various κ ($= p^j_i = s^j_i$). We see that $\kappa > 0$ gives a better performance (i.e. negative real part eigenvalues for the constraint propagation equation), while excessively large positive κ makes the system divergent again.

3.3. Example 2: Einstein equations (Ashtekar equations)

3.3.1. Adjusted system for controlling constraint violations. Here we only consider the adjusted system which controls the departures from the constraint surface. In the appendix, we present an advanced system which controls the violation of the reality condition together with a numerical demonstration.

Even if we restrict ourselves to adjusted equations of motion for $(\tilde{E}_a^i, \mathcal{A}_i^a)$ with constraint terms (no adjustment with derivatives of constraints), generally, we could adjust them as

$$\partial_t \tilde{E}_a^i = -i\mathcal{D}_j(\epsilon^{cb} \tilde{N} \tilde{E}_c^j \tilde{E}_b^i) + 2\mathcal{D}_j(N^{[j} \tilde{E}_a^{i]}) + i\mathcal{A}_0^b \epsilon_{ab}{}^c \tilde{E}_c^i + X_a^i \mathcal{C}_H + Y_a^{ij} \mathcal{C}_{Mj} + P_a^{ib} \mathcal{C}_{Gb}, \quad (3.14)$$

$$\partial_t \mathcal{A}_i^a = -i\epsilon^{ab}{}^c \tilde{N} \tilde{E}_b^j F_{ij}^c + N^j F_{ji}^a + \mathcal{D}_i \mathcal{A}_0^a + \Lambda \tilde{N} \tilde{E}_i^a + Q_i^a \mathcal{C}_H + R_i^{ja} \mathcal{C}_{Mj} + Z_i^{ab} \mathcal{C}_{Gb}, \quad (3.15)$$

where $X_a^i, Y_a^{ij}, Z_i^{ab}, P_a^{ib}, Q_i^a$ and R_i^{ja} are multipliers. However, in order to simplify the discussion, we restrict multipliers so as to reproduce the symmetric hyperbolic equations of motion [10, 11], i.e.

$$\begin{aligned} X &= Y = Z = 0, \\ P_a^{ib} &= \kappa_1(N^i \delta_a^b + i\tilde{N} \epsilon_a{}^{bc} \tilde{E}_c^i), \\ Q_i^a &= \kappa_2(e^{-2} \tilde{N} \tilde{E}_i^a), \\ R_i^{ja} &= \kappa_3(i e^{-2} \tilde{N} \epsilon^{ac}{}^b \tilde{E}_i^b \tilde{E}_c^j). \end{aligned} \quad (3.16)$$

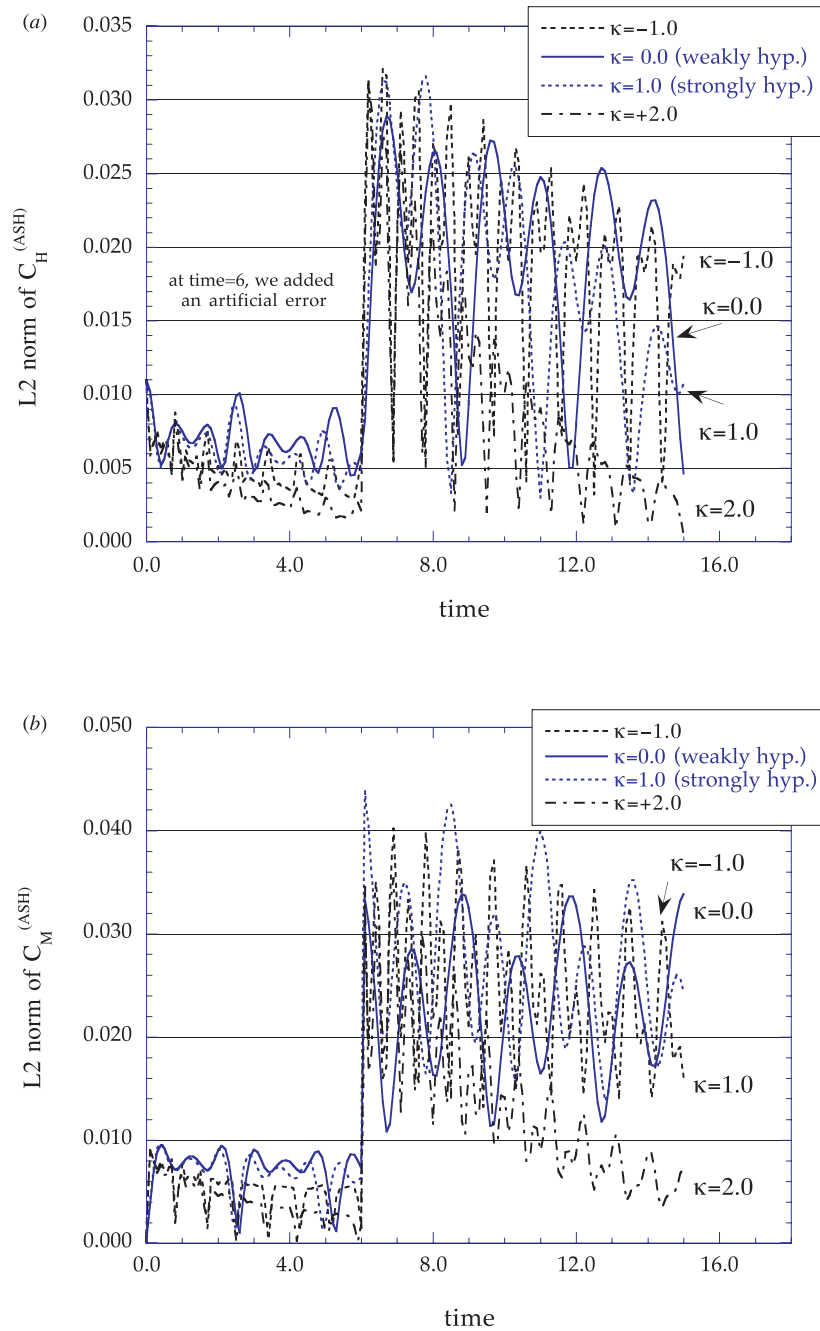


Figure 5. Demonstration of the adjusted system in the Ashtekar equation. We plot the violation of the constraint for the same model as figure 3(b). An artificial error term was added at $t = 6$, in the form of $\mathcal{A}_y^2 \rightarrow \mathcal{A}_y^2(1 + \text{error})$, where error is +20% as before. (a), (b) L2 norm of the Hamiltonian constraint equation, C_H , and momentum constraint equation, C_{M_x} , respectively. The full curve is the case of $\kappa = 0$, that is the case of ‘no adjusted’ original Ashtekar equation (weakly hyperbolic system). The dotted curve is for $\kappa = 1$, equivalent to the symmetric hyperbolic system. We see that the other curve ($\kappa = 2.0$) shows better performance than the symmetric hyperbolic case.

Here $\kappa_1 = \kappa_2 = \kappa_3 = 1$ is the case of a symmetric hyperbolic equation for $(\tilde{E}_a^i, \mathcal{A}_i^a)$, while $\kappa_1 = \kappa_2 = \kappa_3 = 0$ is the (Ashtekar's original) weakly hyperbolic equation, and other choices of κ s let the equation satisfy the level of strongly hyperbolic form.

With these adjusted terms, the constraint propagation equations become

$$\partial_t^{(1)}\mathcal{C}_H = (1 - 2\kappa_3)(\partial_j^{(1)}\mathcal{C}_{Mj}), \quad (3.17)$$

$$\partial_t^{(1)}\mathcal{C}_{Mi} = (1 - 2\kappa_2)(\partial_i^{(1)}\mathcal{C}_H) + i\kappa_3\epsilon^{mj}_i(\partial_m^{(1)}\mathcal{C}_{Mj}), \quad (3.18)$$

$$\partial_t^{(1)}\mathcal{C}_{Ga} = -2\kappa_3^{(1)}\mathcal{C}_{Ma} + i\kappa_1\epsilon_a^{bm}(\partial_m^{(1)}\mathcal{C}_{Gb}), \quad (3.19)$$

against the Minkowskii background. The eigenvalues of the coefficient matrix after the Fourier transformation are

$$(0, \pm i\kappa_1\sqrt{k^2}, \pm i\kappa_3\sqrt{k^2}, \pm i(2\kappa_2 - 1)(2\kappa_3 - 1)\sqrt{k^2}) \quad (3.20)$$

where $k^2 := k_i k^i$. For example,

$$(0 \text{ (multiplicity 5)}, \pm i\sqrt{k^2}) \quad \text{for } \kappa_1 = \kappa_2 = \kappa_3 = 0: \quad \text{original system} \quad (3.21)$$

$$(0 \text{ (multiplicity 3)}, \pm i\sqrt{k^2} \text{ (multiplicity 3)})$$

$$\text{for } \kappa_1 = \kappa_2 = \kappa_3 = 1: \quad \text{symmetric hyperbolic system.} \quad (3.22)$$

That is, our guideline (b) is obtained.

The above adjustment, (3.14)–(3.16), will not produce negative real part eigenvalues, so our guideline (a) cannot be applied here. If we adjust the dynamical equation using the spatial derivatives of constraint terms, then it is possible to get all negative eigenvalues like in the Maxwell system (though this is complicated). However, since we found that this adjustment, (3.14)–(3.16), gives us an example of controlling the violation of the constraint equations for our purpose, we only show this simpler version here.

3.3.2. Numerical demonstration. As a demonstration, here we use the same model as in section 2.3.3, that is, gravitational wave propagation in the plane-symmetric spacetime, with an artificial error in the middle of the time evolution. We examine how the adjusted multipliers contribute to the system's stability. In figure 5, we show the results of this experiment. We plot the violation of the constraint equations, both \mathcal{C}_H and \mathcal{C}_{Mx} . An artificial error term was added at $t = 6$, as a kick of $\mathcal{A}_y^2 \rightarrow \mathcal{A}_y^2(1 + \text{error})$, where the error amplitude is +20% as before. We set $\kappa \equiv \kappa_1 = \kappa_2 = \kappa_3$ for simplicity. The full curve is the case of $\kappa = 0$, that is the case of 'no adjusted' original Ashtekar equation (weakly hyperbolic system). The dotted curve is for $\kappa = 1$, equivalent to the symmetric hyperbolic system. We see that the other curve ($\kappa = 2.0$) shows better performance than the symmetric hyperbolic case.

4. Discussion

With the purpose of searching for an evolution system of the Einstein equations which is robust against perturbative errors for the free evolution of the initial data, we studied two 'asymptotically constrained' systems.

First, we examined the previously proposed ' λ system', which introduces artificial flows to constraint surfaces based on the symmetric hyperbolic formulation. We showed that this system works as expected for the wave propagation problem in the Maxwell system and in Ashtekar's system of general relativity. However, the λ system cannot be applied to *general* dynamical systems in general relativity, since the system requires the base system to be symmetric hyperbolic form.

Alternatively, we proposed a new mechanism to control the stability, which we called the ‘adjusted system’. This is simply obtained by adding constraint terms in the dynamical equations and adjusting the multipliers. We proposed two guidelines for specifying multipliers which reduce the numerical errors; that is, non-positive real-part or pure-imaginary eigenvalues of the adjusted constraint propagation equations. This adjusted system was also tested in the Maxwell and Ashtekar’s system.

As we denoted earlier, the idea of adding constraint terms is not new. However, we think that our guidelines for controlling the decay of constraint equations are appropriate for our purposes, and were not suggested before. Up to our numerical experiments, our guidelines give us clear indications as to whether the constraints decay (i.e. a stable system) or not for perturbative errors, though we also think that this is not a complete explanation for all cases. This feature may be explained or proven in different ways, such as the finiteness of the norm (of evolution equations or of constraint propagation equations), or by another mechanism in the future.

Our secondary conclusion is that the symmetric hyperbolic equation is not always the best one for controlling stable evolution. As we show in the wave propagation model in the adjusted Ashtekar equation, our eigenvalue guidelines affect more than the system’s hyperbolicity. (We found a similar conclusion in [16].) We think that this result opens a new direction to numerical relativists for future treatment of the Einstein equations.

We are now applying our idea to the standard ADM and conformally scaled ADM system to explain these differences. Results will be reported elsewhere [17].

Acknowledgments

HS appreciates helpful comments by Abhay Ashtekar, Jorge Pullin, Douglas Arnold and L Samuel Finn, and the hospitality of the CGPG group. We thank Bernard Kelly for a careful reading the manuscript. Numerical computations were performed using machines at CGPG. This work was supported in part by the NSF grant PHYS98-00973, and the Everly research funds of Penn State. HS was supported by the Japan Society for the Promotion of Science as a research fellow abroad.

Appendix A. Controlling the reality condition using an adjusted system

We demonstrate here that our adjusted system in the Ashtekar formulation also works for controlling reality conditions. As a model problem, we look at the degenerate point passing problem which we considered previously in [18]. In section A.1, we review this background briefly, and in section A.2 we show our numerical demonstrations.

A.1. Degenerate point passing problem

In [18], the authors had examined the possibility of dynamical passing of the degenerate point in the spacetime. There the authors found that we are able to pass (i.e. continue time evolutions) if we could foliate the time-constant hypersurface into a complex plane assuming that such a degenerate point exists on the real plane. Such foliations are available within Ashtekar’s original formulation, since the fundamental variables are complex quantities. The trick is to violate the reality condition locally, only in the vicinity of a degenerate point.

As a model, we construct a metric, ${}^{(4)}g$, which possesses a degenerate point ($\det {}^{(3)}g = 0$) at the origin $t = x = 0$ in the Minkowskii background metric:

$$\begin{aligned} ds^2 = & -[1 - (2tx \exp(-t^2 - x^2))^2] dt^2 \\ & + 4tx \exp(-t^2 - x^2)[1 - (1 - 2x^2) \exp(-t^2 - x^2)] dt dx \\ & + [1 - (1 - 2x^2) \exp(-t^2 - x^2)]^2 dx^2 + dy^2 + dz^2. \end{aligned} \quad (\text{A.1})$$

We consider the time evolution for which initial data are described by a particular time slice $t < 0$ of (A.1), and whose time-constant hypersurfaces are foliated by the gauge condition,

$$N = 1 \quad (\tilde{N} = e^{-1}), \quad (\text{A.2})$$

$$N_x = 2tx \exp(-t^2 - x^2)[1 - (1 - 2x^2) \exp(-t^2 - x^2)] + iat \exp(-b(t^2 + x^2)), \quad (\text{A.3})$$

$$\mathcal{A}_0^a = 0, \quad (\text{A.4})$$

which enables our detour into the complex plane. Our goal is to demonstrate that the time evolution comes back to the real plane without any divergence in variables and curvatures. Such a ‘recovering condition’ can be described by

$$\left. \begin{aligned} \int_{t_-}^{t_+} \text{Im } N(t, \mathbf{x}) dt = 0, \\ \int_{t_-}^{t_+} \text{Im } N^i(t, \mathbf{x}) dt = 0, \end{aligned} \right\} \quad \text{foliation recovering condition} \quad (\text{A.5})$$

$$\left. \begin{aligned} \text{Im } N(t, \mathbf{x}) \rightarrow 0, \\ \text{Im } N^i(t, \mathbf{x}) \rightarrow 0, \\ \text{Im} [\tilde{E}_a^i \tilde{E}^{ja} / \det \tilde{E}(t, \mathbf{x})] \rightarrow 0, \end{aligned} \right\} \quad \text{asymptotic reality condition} \quad (\text{A.6})$$

for all four limits $\mathbf{x} \rightarrow \mathbf{x}_* \pm \Delta \mathbf{x}$, $t \rightarrow t_* \pm \Delta t$.

Numerically, this problem becomes an eigenvalue problem, since our boundary conditions, (A.5) and (A.6), specify much freedom. To see whether the evolution satisfies the criteria or not, we introduced two measures

$$F(t_{final}) := \max_x |\text{Re}(e(t = t_{final}, x) - 1)| \quad (\text{asymptotically flat}) \quad (\text{A.7})$$

$$R(t_{final}) := \max_x |\text{Im}(e(t = t_{final}, x))| \quad (\text{asymptotically real}) \quad (\text{A.8})$$

and searched the parameters a and b in (A.3).

If we apply our adjusted system to this model, then we expect that the allowed range for the parameters a and b becomes more general, since the real-surface-recovering feature is in the flow of the adjusted system’s foliation.

A.2. Application of the adjusted system

As was shown in the previous section, for this purpose, we have to foliate our hypersurface in the complex-valued region and foliate back to the real-valued surface. That is, we can treat the reality condition, both primary and secondary, as being part of the constraint equations.

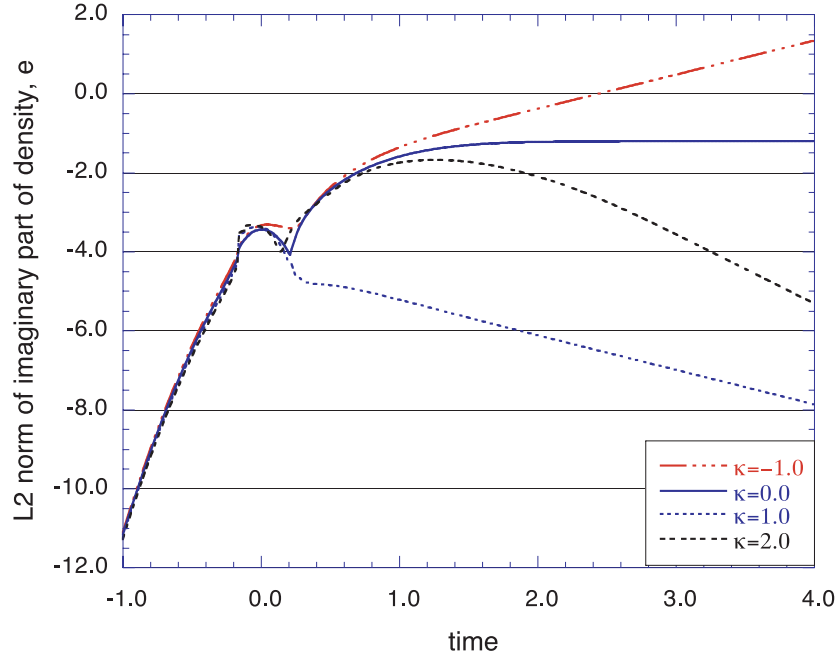


Figure A1. Demonstration of the adjusted system to control the reality condition in the Ashtekar formulation. Reality violation (L2 norm of the imaginary part of the density) versus time are plotted for various adjusted coefficient $\kappa = -1, 0, 1, 2$. We see that $\kappa > 0$ has better performance (negative real-part eigenvalues of the reality propagation equation, (A.11)).

For the above degenerate point-passing problem, we need to control only the violation of $\text{Im}(\tilde{E}_a^i \tilde{E}_a^j)$. Therefore, similar to the proposal of the adjusted system discussed in section 2.3, our adjusted dynamical equations can be written as

$$\begin{aligned} \partial_t \tilde{E}_a^i = & -i\mathcal{D}_j(\epsilon^{cb} N_{\sim} \tilde{E}_c^j \tilde{E}_b^i) + 2\mathcal{D}_j(N^{[j} \tilde{E}_a^{i]}) + i\mathcal{A}_0^b \epsilon_{ab}{}^c \tilde{E}_c^i + X_a^i \mathcal{C}_H + Y_a^{ij} \mathcal{C}_{Mj} + P_a^{ib} \mathcal{C}_{Gb} \\ & + T^i{}_{ajk} \text{Im}(\tilde{E}_b^j \tilde{E}_b^k), \end{aligned} \quad (\text{A.9})$$

$$\begin{aligned} \partial_t \mathcal{A}_i^a = & -i\epsilon^{ab} N_{\sim} \tilde{E}_b^j F_{ij}^c + N^j F_{ji}^a + \mathcal{D}_i \mathcal{A}_0^a + \Lambda N_{\sim} \tilde{E}_i^a + Q_i^a \mathcal{C}_H + R_i^{aj} \mathcal{C}_{Mj} + Z_i^{ab} \mathcal{C}_{Gb} \\ & + V^a{}_{ijk} \text{Im}(\tilde{E}_b^j \tilde{E}_b^k), \end{aligned} \quad (\text{A.10})$$

where $X_a^i, Y_a^{ij}, Z_i^{ab}, P_a^{ib}, Q_i^a, R_i^{aj}, T^i{}_{ajk}$ and $V^a{}_{ijk}$ are adjusted multipliers.

If we simply set $X_a^i = Y_a^{ij} = Z_i^{ab} = P_a^{ib} = Q_i^a = R_i^{aj} = V^a{}_{ijk} = 0$ and $T^i{}_{ajk} = -i\kappa \delta_j^i \delta_{ak}$ (where κ is a real constant), then we obtain the constraint propagation equation

$$\partial_t^{(0)} \text{Im}(\tilde{E}_a^i \tilde{E}_a^j) = -2\kappa^{(0)} \text{Im}(\tilde{E}_a^i \tilde{E}_a^j) + \text{other constraint terms}. \quad (\text{A.11})$$

The eigenvalue of the Fourier-transformed right-hand side is -2κ . That is, if we set $\kappa > 0$ (< 0) then the eigenvalue is negative (positive), while $\kappa = 0$ recovers the original non-adjusted system.

The results of the numerical demonstration are shown in figure A1. We plot the L2 norm of the violation of the reality condition as a function of time, t (this evolution is from $t = -5$ to 5 [18]). Around the time $t = 0$ the error appears due to our ‘detour’ slicing condition, and

the original system ($\kappa = 0$) will not recover the reality surface with the choice of a and b in (A.3) for this plot. However, for the positive κ case, the foliation will be forced to recover the reality surface, while for the negative κ case it will not.

Therefore, this example again supports our guidelines, i.e. a negative eigenvalue of the constraint propagation equation will guarantee the evolution to the constraint surface.

Appendix B. von Neumann analysis of constraint propagation equations

Here we show von Neumann's stability analysis for the constraint propagation equations, in order to support our guideline (3b) for the adjusted system (section 3.1). The von Neumann analysis (see, e.g., [19]) gives us powerful predictions for the stability of a finite-difference approximation. Briefly, the analysis consists of a Fourier decomposition in the spatial directions of the dynamical variables and its one-step time evolution with a particular time integration scheme. If we wrote the fundamental variable $\phi(x, t)$, then the criteria for the stability is $|\lambda_i| \leq 1$ where λ_i are the eigenvalues of the amplification matrix G , which is in the expression of the evolution equations in the form of $\phi(x, t + \Delta t) = G\phi(x, t)$.

In our discussion, the constraint propagation equations are not directly used for numerical integrations, but are used as a guideline for the stability. The application of von Neumann analysis, however, is also allowed for the constraint propagation equations, as far as substituting the finite derivatives in the analysis using those of the fundamental dynamical variables. Here we show the simplest cases for the adjusted Maxwell system and the adjusted Ashtekar system.

Adjusted Maxwell system. We start by choosing $\kappa := P_1 = P_2 = P_3$ with other multipliers zero in the system (3.7) and (3.8). The Fourier component of the propagation equation for C_E (3.11) becomes $\partial_t \hat{C}_E = i\kappa(k_x + k_y + k_z)\hat{C}_E$, for which the eigenvalue (3.13) is $i\kappa(k_x + k_y + k_z)$. That is, non-zero κ gives us a pure-imaginary eigenvalue. By applying von Neumann analysis, we obtain the amplitude G s for FTCS (forward time and centre space difference), Brailovskaya and (two-iteration) iterative Crank Nicholson schemes as

$$|G_{FTCS}|^2 = 1 + (\kappa\sigma)^2, \quad (\text{B.1})$$

$$|G_{Br}|^2 = 1 - (\kappa\sigma)^2 + (\kappa\sigma)^4, \quad (\text{B.2})$$

$$|G_{CN2}|^2 = 1 - (\kappa\sigma)^4/4 + (\kappa\sigma)^6/16, \quad (\text{B.3})$$

respectively, where $\sigma = (\Delta t/\Delta x)(\sin(k_x \Delta x) + \sin(k_y \Delta x) + \sin(k_z \Delta x))$ and we assume a three-dimensional finite grid of equal spacing Δx in all directions. Except for the FTCS scheme, we see that non-zero $|\kappa|$ (near $\kappa = 0$) yields $|G| < 1$. The bigger $|\kappa|$ (near $\kappa = 0$) gives less $|G| < 1$. The simulation we showed in section 3.2 is not this case (since we tried to show the one which satisfy guideline (3a)), but we also obtained numerical results which confirm our conjecture here.

Adjusted Ashtekar system. Similarly, for the constraint propagation equations (3.17)–(3.19), with $\kappa := \kappa_1 = \kappa_2 = \kappa_3$, we obtain the eigenvalues λ_i of the amplification matrix G for the above three schemes,

$$|\lambda_{FTCS}|^2 = 1, \quad 1 + (\kappa\sigma)^2, \quad 1 + \{(1 - 2\kappa)(\kappa\sigma)\}^2, \quad (\text{B.4})$$

$$|\lambda_{Br}|^2 = 1, \quad 1 - (\kappa\sigma)^2 + (\kappa\sigma)^4, \quad 1 - \{(1 - 2\kappa)\sigma\}^2 + \{(1 - 2\kappa)\sigma\}^4, \quad (\text{B.5})$$

$$|\lambda_{CN2}|^2 = 1, \quad 1 - (\kappa\sigma)^4/4 + (\kappa\sigma)^6/16, \quad 1 - \{(1 - 2\kappa)\sigma\}^4/4 + \{(1 - 2\kappa)\sigma\}^6/16, \quad (\text{B.6})$$

with multiplicity 1, 4 and 2, respectively. Here again we see that non-zero $|\kappa|$ makes the system $|G| < 1$ for Brailovskaya and two-iteration Crank–Nicholson schemes. This analysis supports why guideline (3b) works for our results shown in figure 5.

References

- [1] Shinkai H and Yoneda G 2000 *Class. Quantum Grav.* **17** 4899
- [2] Bona C and Massó J 1992 *Phys. Rev. Lett.* **68** 1097
Bona C, Massó J, Seidel E and Stela J 1995 *Phys. Rev. Lett.* **75** 600
Bona C, Massó J, Seidel E and Stela J 1997 *Phys. Rev. D* **56** 3405
- [3] Choquet-Bruhat Y and York J W Jr 1995 *C. R. Acad. Sci., Paris I* **321** 1089
(Choquet-Bruhat Y and York J W Jr 1995 *Preprint gr-qc/9506071*)
Abrahams A, Anderson A, Choquet-Bruhat Y and York J W Jr 1995 *Phys. Rev. Lett.* **75** 3377
Abrahams A, Anderson A, Choquet-Bruhat Y and York J W Jr 1996 *C. R. Acad. Sci., Paris IIb* **323** 835
Abrahams A, Anderson A, Choquet-Bruhat Y and York J W Jr 1997 *Class. Quantum Grav.* **14** A9
Anderson A and York J W Jr 1999 *Phys. Rev. Lett.* **82** 4384
- [4] Friedrich H 1981 *Proc. R. Soc. A* **375** 169
Friedrich H 1981 *Proc. R. Soc. A* **378** 401
Friedrich H 1985 *Commun. Math. Phys.* **100** 525
Friedrich H 1991 *J. Diff. Geom.* **34** 275
Friedrich H 1996 *Class. Quantum Grav.* **13** 1451
- [5] Frittelli S and Reula O A 1996 *Phys. Rev. Lett.* **76** 4667
See also Stewart J M 1998 *Class. Quantum Grav.* **15** 2865
- [6] van Putten M H P M and Eardley D M 1996 *Phys. Rev. D* **53** 3056
- [7] Ashtekar A 1986 *Phys. Rev. Lett.* **57** 2244
Ashtekar A 1987 *Phys. Rev. D* **36** 1587
Ashtekar A 1991 *Lectures on Non-Perturbative Canonical Gravity* (Singapore: World Scientific)
- [8] Brodbeck O, Frittelli S, Hübner P and Reula O A 1999 *J. Math. Phys.* **40** 909
- [9] Shinkai H and Yoneda G 1999 *Phys. Rev. D* **60** 101502
- [10] Yoneda G and Shinkai H 1999 *Phys. Rev. Lett.* **82** 263
- [11] Yoneda G and Shinkai H 2000 *Int. J. Mod. Phys. D* **9** 13
- [12] Detweiler S 1987 *Phys. Rev. D* **35** 1095
- [13] Nakamura T, Oohara K and Kojima Y 1987 *Prog. Theor. Phys. Suppl.* **90** 1
Shibata M and Nakamura T 1995 *Phys. Rev. D* **52** 5428
See also, Baumgarte T W and Shapiro S L 1999 *Phys. Rev. D* **59** 024007
- [14] Frittelli S 1997 *Phys. Rev. D* **55** 5992
- [15] Alcubierre M, Allen G, Brügmann B, Seidel E and Suen W M 2000 *Phys. Rev. D* **62** 124011
- [16] Hern S D 2000 *PhD Thesis Preprint gr-qc/0004036*
- [17] Yoneda G and Shinkai H, in preparation
- [18] Yoneda G, Shinkai H and Nakamichi A 1997 *Phys. Rev. D* **56** 2086
- [19] Richtmyer R D and Morton K W 1967 *Difference Methods for Initial-Value Problems* 2nd edn (New York: Wiley)